Journal of Materials Science and Chemical Engineering, 2026, 14(11), 59-81
https://www.scirp.org/journal/msce
ISSN Online: 2327-6053
ISSN Print: 2327-6045

An Experimental Investigation into Altering the Surface Microgeometry of Tungsten Electrodes

Dorin Guzgan[1,2], Pavel Topala[1,2]

[1]Department of Manufacturing Technology, National University of Science and Technology POLITEHNICA Bucharest, Bucharest, Romania
[2]Department of Physical and Engineering Sciences, Alecu Russo Balti State University, Balti, Republic of Moldova
Email: pavel.topala@gmail.com

How to cite this paper: Guzgan, D. and Topala, P. (2026) An Experimental Investigation into Altering the Surface Microgeometry of Tungsten Electrodes. *Journal of Materials Science and Chemical Engineering*, **14**, 59-81.
https://doi.org/10.4236/msce.2026.1411004

Received: July 29, 2026
Accepted: November 23, 2026
Published: November 26, 2026

Copyright © 2026 by author(s) and Scientific Research Publishing Inc.
This work is licensed under the Creative Commons Attribution International License (CC BY 4.0).
http://creativecommons.org/licenses/by/4.0/
Open Access

Abstract

This study investigates the formation of conical micro-protrusions on metallic surfaces subjected to individual pulsed electrical discharges. The experiments showed that the polarity of the processed electrode has a significant influence on the formation of conical surface structures, with a more pronounced effect observed when the workpiece is connected as the anode of the pulsed-current discharge circuit. The obtained results also indicate that the geometry of the resulting micro-protrusions is affected by the relative position of the electrodes and by the forces acting on the transient liquid phase during the discharge process. Conical structures were obtained on the surfaces of tungsten, tungsten-rhenium and other metallic materials, demonstrating the applicability of pulsed electrical discharges for controlled modification of conductive surfaces. The dimensions and morphology of the resulting micro-protrusions are associated with the properties and composition of the processed material, the interelectrode gap, the energy released during the discharge, and the pulse duration. The experimental findings provide a basis for establishing technological conditions for the controlled modification of metallic surface microgeometry through the formation of Taylor-cone-type asperities.

Keywords

Impulse, Gap, Microgeometry, Electrode, Cathode, Emission

1. Introduction

Driven by recent advancements in micro- and nanoelectronics, the issue of increasing the active surface area of device components used in various fields and constructions has become highly relevant. A special role in this context is attributed to the intentional modification of the geometry of active surfaces, in par-

ticular the creation of micro-protrusions with specific geometries [1]-[4]. Workpieces featuring surface conical micro-protrusions display functional characteristics distinct from the parent substrate, largely driven by their specific geometric architecture. Consequently, they are highly promising for a wide range of applications, including, but not limited to solar cells, surface-enhanced Raman spectroscopy [5], and field emitters [6] [7], making this approach both viable and practical. The author [8], who studied the processes of generating metallic ions, established that these simultaneously act as droplet emitters, and that the quantity of expelled ions and droplets depends heavily on Taylor cone geometry. Employing both an analytical framework and experimental validation, the findings confirmed that the base radius of the Taylor cone directly determines the rate of droplet formation in low-impedance emitters. This correlation holds significant implications for optimising emitters for either low or high droplet emission rates at different emission current intensities [8].

In the paper [9], the authors investigated the evaporation process of high-power ions and noted that the presence of micro-protrusions on the active surface leads to a marked enlargement of droplet generation diameter on the conical meniscus due to the electric field of the space charge.

The authors of the paper [10] analyse the behaviour of surfaces bounded by Taylor cones under the operating conditions of electric field concentrators in spacecraft thrusters. These micro-protrusions are obtained by applying single-wave electric fields, and the oscillation period strongly affects the correlation between the cone's diameter and angle, which in turn influences the relaxation time of the liquid charge.

In a related study, [11] described template-free pulse electrodeposition as a viable method for fabricating densely packed vertical copper (Cu) microcone arrays. The morphological features of these nanotwinned Cu (nt-Cu) microcones closely mirror those depicted in **Figure 1**. Developing nt-Cu microstructures broadens the utility of nanotwinned materials, offering substantial potential for 3D electronic packaging. Furthermore, within the post-Moore paradigm, direct Cu-Cu bonding has emerged as a compelling substitute for traditional solder interconnects in next-generation electronic packaging.

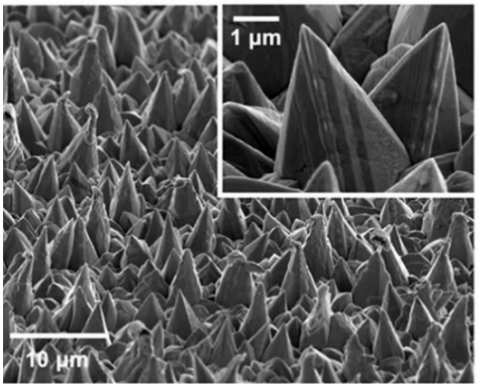

Figure 1. Morphology of nanotwinned Cu (nt-Cu) microcones [11].

Thus, according to source [12], the obtuse polygonal pyramidal microcones (see Figure 2), characterized by a cross-section that increases from tip to base, combined with inherent mechanical properties, induce a high applied stress at the microcone tip and a low yield stress, thereby facilitating the initiation and propagation of plastic deformation during the bonding process. This study demonstrated the feasibility of using Cu microcones for low-temperature bonding without CMP treatment, providing valuable insights into advanced interconnection technologies.

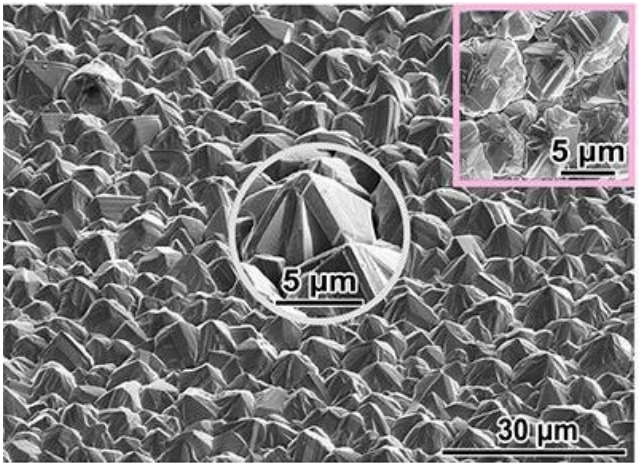

Figure 2. Obtuse polygonal pyramidal microcones [12].

In the paper [13], it is mentioned that under specific conditions, an electric field deforms the free surface of a conductive liquid into a cone, releasing a stable, narrow, current-carrying jet from its apex. The fluid dynamics within the cone-to-jet transition zone are analyzed assuming that its characteristic dimension is negligible relative to all other length scales in the conical meniscus system. Thus, in the work [14], it is reported that applied cones generate electrosprays of highly conductive fluids, where operation in the cone-jet mode produces charged nanodroplets of controllable size and molecular ions. Experimental characterization yields comprehensive data on beam composition alongside jet parameters. Specifically, the beam comprises primary ions generated by jet disintegration, secondary ions produced via desolvation, stable primary droplets formed during breakup, smaller offspring droplets resulting from Coulomb explosions of unstable droplets, and small primary droplets that lose a substantial fraction of their charge through evaporation during flight. In authors' paper [15], the formation of asperities during electrochemical discharge machining (ECDM) was reported; however, the authors did not highlight them for technological purposes nor attempted to explain the phenomenon of their formation. From the above, it follows that the modification of surface microgeometry holds significant promise for next-generation technology development. For this reason, the authors of the present work decided to revisit surface machining using pulsed electrical discharges (PED).

Analysis of experimental results reported by several authors [1] [6] [7] [16]-

[23] has shown that when machining metallic surfaces with pulsed electrical discharges, material removal occurs along with the formation of spherical-cap-shaped craters [1] [6] [7] [17]-[20]. Morphological alteration of the processed metal substrates is caused by the action of "cold" electron spots (without evident signs of melting) and "hot" spots (which generate abundant liquid phase) [1] [6] [7] [20]-[25]. It was observed that craters form in areas of the electrode surface with increased electric field intensity; for a relatively small number of discharges, the effect is more pronounced on electrode surfaces connected as anodes [1] [6] [18] [19] [23]. Once formed, craters promote the formation of new craters due to the significant increase in electric field intensity at the edges of existing ones [6] [7] [20]. The crater formation mechanism remains largely unclear.

According to several authors [1] [6] [7] [20] [23]-[26], three types of spherical-cap-shaped craters have been identified: the first exhibiting a smooth surface profile, the second featuring surface roughness, and the third possessing a central conical protrusion. The present study focuses on investigating the conditions leading to the occurrence of the third type of crater (with a central conical asperity), how exactly the microgeometry of the active surface is modified [1] [6] [18] [19] [23] [27]-[29], and how this modification of the active surface microgeometry influences the thermoelectronic emission process of metallic cathodes [30]-[32]. Advancements in manufacturing technologies demand metallic materials with enhanced surface characteristics. According to [33], nano-sized dispersed WC particles with nickel were successfully obtained by electro-codeposition. Conical micro-features were detected at the crater peripheries as well as within their central regions. [2] [18] [19] [23]. In the work [34], referred to as ectons, such conical structures are recognized as key drivers of electron and ion generation, which strongly and positively affect the phenomenon of electron emission [30]-[32] [34]-[38].

In the opinion of several authors [1] [6] [7] [18]-[20] [23]-[25] [39]-[41], conical micro-protrusions form at crater centers due to liquid metal surface instabilities induced by strong electric fields, surface tension, and secondary gravitational forces. The conditions of cone formation can be analysed in more detail based on works [1] [3] [4] [6] [18]-[20] [33] [39]-[46]. The observation of craters and conical micro-features on metallic electrodes following pulse electrodeposition (PED) validates this technique as an effective method for tailoring both the micro-topography and elemental composition of conductive surfaces. The modification process of the surface microgeometry of metallic parts consists in the fact that, under certain conditions of pulsed electrical discharges, conical asperities, also referred to in the literature as Taylor cones, are formed (extracted) on the surface of these parts, with an apex angle of about 90˚, though this angle may vary by approximately ± 1 or even 2˚ according to the results obtained by several authors [1] [2] [7] [18] [23] [30]-[32] [47].

The increase in functional surface area of parts processed by PED, under established conditions, fundamentally alters the nature of their interaction with the

ambient environment and with other active surfaces they come into contact with. Enlarging the effective surface area directly influences their capacity to emit electrons and ions [34]-[37] [48] [49], as well as to absorb different types of radiation [50]. Furthermore, these conical micro-features act as electric field intensifiers, thereby promoting electron emission (autoemission and thermionic emission) [51].

2. Methodology of Experimental Research

After performing multiple trials, it was observed that following pulsed electrical discharges (PED), under certain energy regimes, conical micro-protrusions can be extracted on the surfaces of both the tool and substrate electrodes. The effect of single-pulse electrical discharges is more pronounced on the surface of the anodic electrode. It was further observed that the height of the extracted conical micro-protrusions is generally greater when the anode is positioned with its processed surface facing downward, fixed from above (see **Figure 3(b)**). This phenomenon can be explained by analysing the directions of the forces acting on the liquid metal, namely: the action of the gravitational force *P*, the force of the electric field *Fe* oriented from anode to cathode and the surface tension force *Ft*, oriented in the opposite direction to *Fe*. When the anode is positioned at the bottom (see **Figure 3(a)**), the same forces act on the liquid metal, but with opposite orientations, except for gravity, which does not change its direction. From this, it follows that when the anode is placed at the top, the gravitational force *P* and the electric field force *Fe* act in the same direction, and the resultant of these three forces is greater in the direction of extracting the conical micro-protrusions.

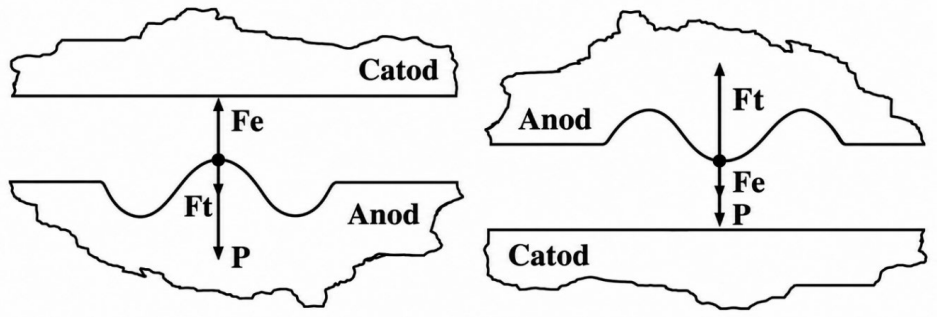

Figure 3. Directions of forces acting on the liquid metal [25].

Thus, it can be noted that at least three types of forces act on the molten metal: gravitational, electrodynamic, and surface tension forces. By analysing the directions of these forces during the machining process, it is more advantageous to position the anode according to variant "b" in **Figure 3** to enhance the extraction of conical micro-protrusions, since the resultant of these forces is directed along the extraction direction. Consequently, the conical micro-protrusions are obtained longer and sharper. Of course, if the goal is not to obtain micro-protrusions

with such shape characteristics, it is recommended to use the anode positioning according to variant "a" in **Figure 3**.

In studies [1] [6] [20] [52]-[55], experimental findings demonstrated that to produce surfaces with micro-protrusions in the form of Taylor cones, the appearance of a liquid phase on the processed surface is necessary, followed by the extraction of the micro-protrusion and ultrarapid solidification of the material in the form of the protrusion. Experimental research demonstrates that, for implementing the technology of surface microgeometry modification through the extraction of Taylor-cone-shaped micro-protrusions, the following conditions must be met:

1) Ensuring local melting of the workpiece, determined by the following relationship (1) [6]:

$$Q = \frac{4W}{\pi \cdot d_C^2 \cdot S} \geq Q_{melt} \tag{1}$$

where Q denotes the heat released within the plasma channel during pulsed electrical discharges (PED); W_s represents the energy liberated in the plasma channel; d_C is the mean diameter of the crater containing a liquid phase formed on the cathode surface; S refers to the interelectrode gap; and Q_{melt} represents the volumetric latent heat of fusion of the workpiece material, determined by the relation $Q_{melt} = q_{melt} \cdot \rho$; where q_{melt} denotes the specific latent heat of fusion and ρ is the density of the workpiece material.

2) An electric field strength of approximately 10^8 V/m is established across the electrode gap [6]:

$$E_{cr} = \sqrt[4]{64\pi^2 \rho g \gamma \cdot 3 \times 10^4} \tag{2}$$

where E_{cr} denotes the critical electric field strength; ρ represents the metal density; g is the gravitational acceleration; and γ corresponds to the surface tension of the molten material. The electric field vector is oriented parallel to the gravitational force.

During the application of pulsed electrical discharges (PED), both the total energy released and its spatial distribution within the plasma discharge column and across the electrode surfaces play a critical role in controlling surface erosion and thermal loading [56]-[58].

Experimental research has shown that the modification of the microgeometry of metallic workpiece surfaces is significantly influenced by parameters such as the composition of the electrode materials, the energy, the gap between the electrodes, and the duration of the discharge pulse. Based on this, certain energy conditions for the extraction of conical micro-protrusions during pulsed electrical discharges (PED) were determined.

For the investigations of surface microgeometry modification through the development of capillary waves on the liquid metal surface [1] [6] [36] [58] [59] under pulsed electrical discharges conditions, an experimental setup was used, consisting of a pulse current generator, a control unit, and a triggering unit.

The authors of [60] highlighted the possibility of obtaining Ni/TiO_2 nanoparti-

cles by electro-codeposition, whereas the research presented in this paper demonstrates the possibility of forming nanostructures and conical micro-protrusions through the application of pulsed electrical discharges.

For comparison, the energy released in the gap ranged from a few hundredths, tenths, or even single joules. The charging voltage of the capacitor bank of the pulse generator could vary between 0 - 240 V, while the capacitance of the generator's capacitor bank was set between 100 - 600 μF (in steps of 100 μF).

Multiple trials showed that the dimensions of the tool electrode play an important role in the extraction of conical micro-protrusions. Specifically, when a cylindrical wire electrode with a small diameter (0.2 mm) is used, these micro-protrusions are obtained much more easily. Another critical parameter is the electrode gap. Experimentally, it was shown that extraction of conical micro-protrusions is most probable at gap sizes up to 0.35 mm, with an optimal range of 0.15 - 0.3 mm. Since the height of the micro-protrusions can reach up to 0.15 mm under pulsed electrical discharges, it is not recommended to set the gap below 0.2 mm in order to avoid micro-welding and short-circuiting. However, if the goal is to obtain conical micro-protrusions at gaps larger than 0.5 mm, much higher energy must be applied. For example, at a 1 mm gap, conical micro-protrusions were obtained only when the pulse generator's capacitor bank was charged to 220 - 240 V and the capacitance was set to 100 - 200 μF. Analysis of the micro-protrusions obtained under these conditions showed that they were not significantly larger than those obtained at lower energies.

3. Experimental Findings on Altering the Surface Micro-Topography of Active Tool Electrodes

According to the methodology described in [1] [6] [36], Taylor cone-shaped asperities (**Figure 4**) were formed on the cylindrical surfaces of pure tungsten and tungsten-rhenium alloy specimens. The workpiece was configured as the anode within the discharge circuit, whereas the tool electrode functioned as the cathode.

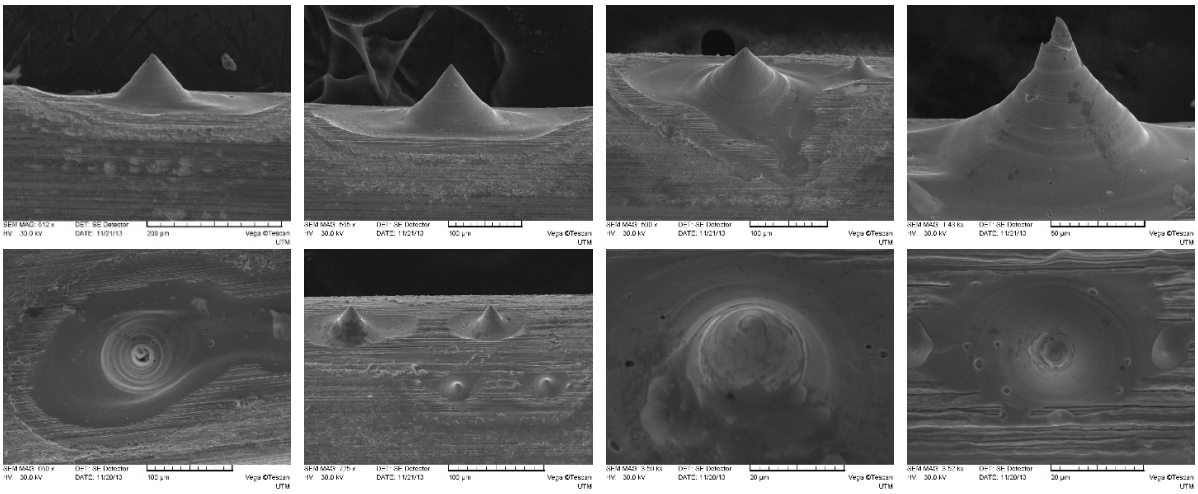

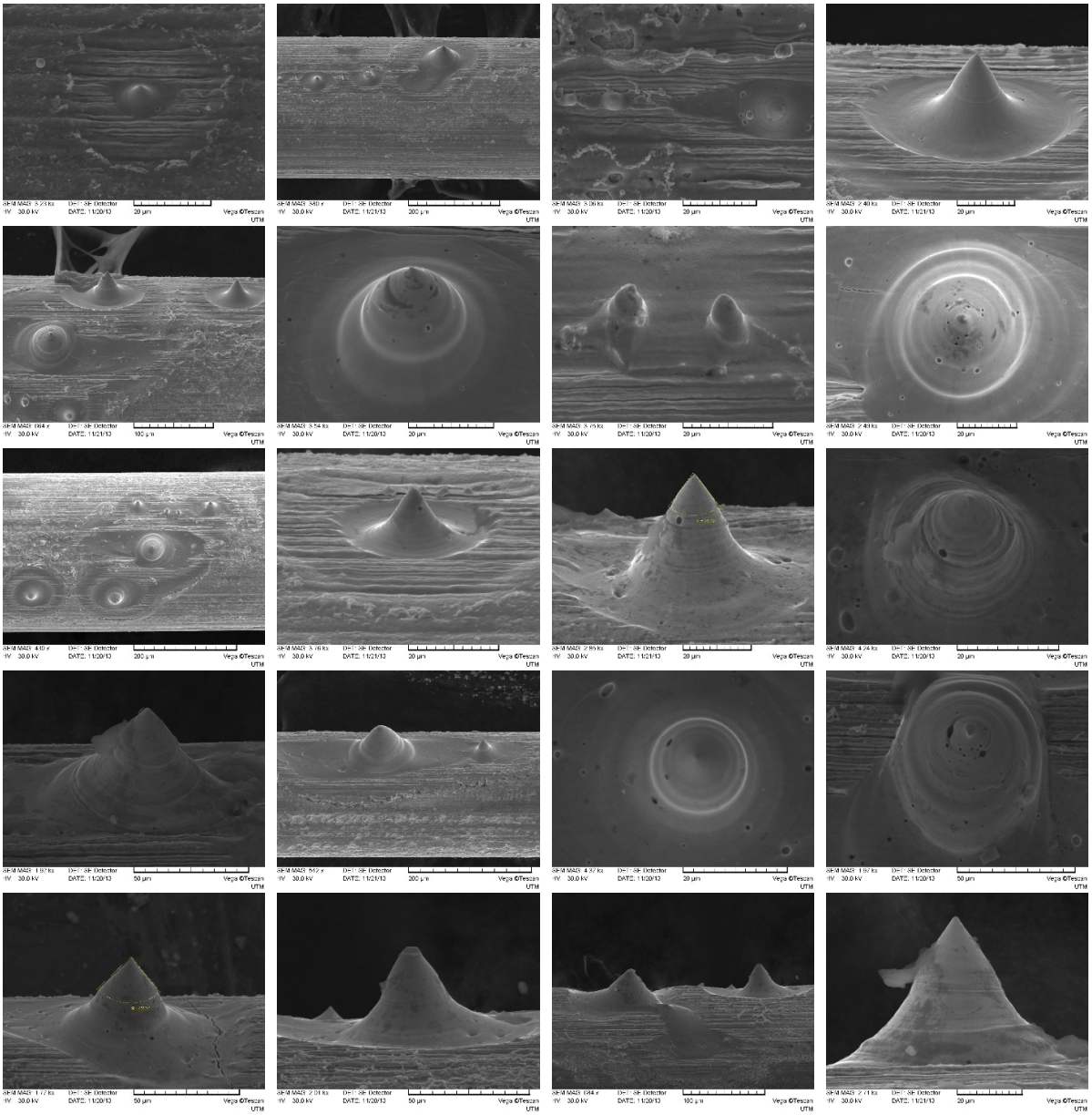

Figure 4. General overview of Taylor cones micro-structures produced by pulsed electrical discharge.

The energetic parameters of the pulsed electrical discharge were: W_c = 0.86 J (energy released in the discharge gap), S = 0.3 mm (gap size), n = 1 (number of electrical discharge pulses per unit surface area). As a result, one or several conical micro-protrusions were extracted from the sample surface (see **Figure 4**).

Experimental investigations analyzed how discharge gap energy release affects anode surface asperity formation when the anode is oriented in the upper position of the circuit. The specimens were manufactured from tungsten of technical purity and from its alloys, such as W + 10% Re and W + 20% Re. To modulate the energy dissipated in the discharge gap, we adjusted the capacitance of the capacitor bank in discrete steps, from a minimum value of 100 μF up to a maximum of 600 μF. Multiple experimental trials were performed to enhance the statistical ac-

curacy of the findings. Observations demonstrated that for the W+ 10% Re alloy, with the increase of energy in the capacitor bank from 0.072 J to 0.432 J, the height of the micro-protrusions varied from 51 μm to 123 μm, while for specimens made of tungsten of technical purity, their height varied from 29 μm to 71 μm. Using an oscilloscope, peak pulse current and pulse duration were recorded as a function of the pulse generator's capacitor bank capacitance (see Table 1 and Table 2).

Table 1. Influence of discharge gap energy and pulse duration on the meniscus base diameter and height for a W+ 10% Re alloy substrate.

Nr.	S, mm	C, μF	U_c, V	I_m, A	W_s, J	τ, μs	h_m, μm	$d_{b.m.}$, μm
1.	0.25	100	60	94	0.072	100	51	83
2.		200	60	125	0.144	125	72	89
3.		300	60	151	0.216	160	86	110
4.		400	60	163	0.288	180	97	139
5.		500	60	172	0.36	200	109	170
6.		600	60	177	0.432	220	123	195

Table 2. Influence of discharge gap energy and pulse duration on the meniscus base diameter and height for a tungsten substrate.

Nr.	S, mm	C, μF	U_c, V	I_m, A	W_s, J	τ, μs	h_m, μm	$d_{b.m.}$, μm
1.	0.2	100	60	100	0.072	100	29	55
2.		200	60	144	0.144	125	34	83
3.		300	60	168	0.216	160	41	110
4.		400	60	180	0.288	180	55	134
5.		500	60	186	0.36	200	64	161
6.		600	60	204	0.432	220	71	179

In Figure 5 and Figure 6 are presented the dependencies of the meniscus height and the diameters of the meniscus bases with respect to the energy released in the discharge gap during the PED process. To put it simply, energy released in the discharge gap plays a pivotal role in dictating meniscus formation on metal interfaces.

From the graph shown in Figure 6, it can be observed that for an energy value of 0.216 J, the diameters of the meniscus bases are practically identical for both materials, while in the other cases they differ. In other words, at these energy levels, menisci with identical base diameters but different heights can be obtained on the surfaces of the two materials. The formation of menisci with greater height on the surface of the W+ 10% Re alloy, compared to those formed on the surface of tungsten of technical purity, is explained by the so-called "rhenium effect." Metals such as W and Re have a high melting temperature, are brittle, and in some cases, this limits their applicability. Alloying these metals with Re increases plasticity,

improves wear resistance, lowers the ductile-to-brittle transition temperature, etc.

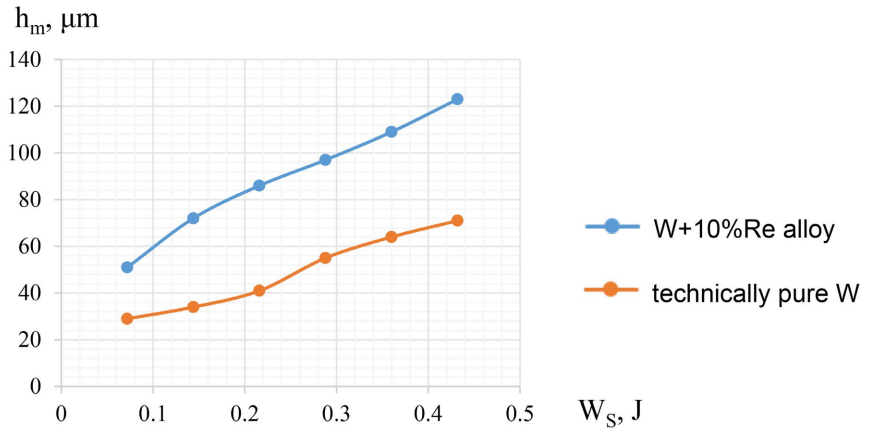

Figure 5. The height of conical meniscus as a function of the energy released in the interstice.

As illustrated by the graphs below, both the height of the menisci and the diameter of their base are strongly influenced by the energy released in the interstice.

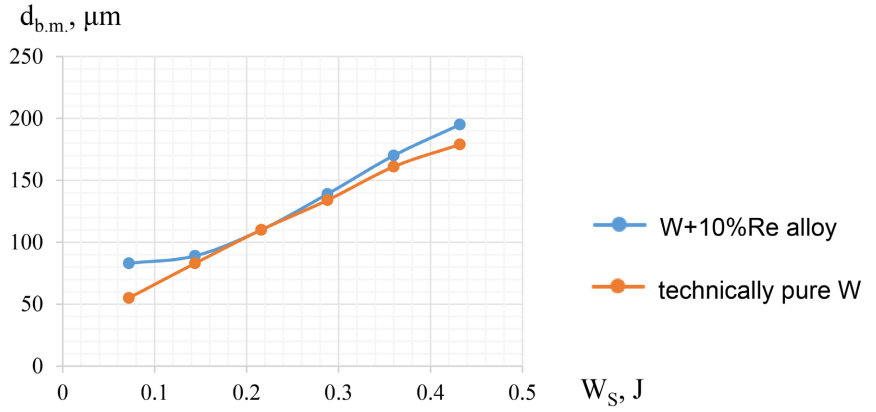

Figure 6. Dependence of meniscus base diameters on the energy released in the interstice [36].

Experimental investigations confirmed that the apex angle of most menisci lies within the range of 88˚ - 92˚. In addition, in some cases, a spherical solidified metal droplet was observed at the tip of the menisci. This indicates that the nanometer-sized droplet was not removed in time and crystallized at the moment of extraction, precisely at the tip of the meniscus. It should be noted that not all menisci exhibit sharp tips. This phenomenon can be explained by the fact that, during pulsed electrical discharges, the extracted meniscus merged with the meniscus formed on the surface of the opposite electrode, *i.e.*, the cathode. Both the geometric parameters of the menisci (Taylor cones) and the electrodynamic parame-

ters (pulse current values, pulse duration, charging voltage of the capacitor bank, voltage drop across the interstice) are presented in Table 3. The potential difference between the electrodes (US) was 21 V.

It should be emphasized that, in determining the influence of the energy stored in the capacitor bank on the geometry of the menisci (Taylor cones), the capacitance of the bank was varied. In turn, the change in capacitance affected the maximum current in the discharge circuit, as well as the corresponding energy and duration of the discharge pulse.

Under pulsed electrical discharges, strong electric field forces trigger the release of discrete or elementary particles from the tips of Taylor cones, overriding the influence of gas bubble pressure drops.

Figure 7 presents the dependence of meniscus height on the energy stored in the capacitor bank (*i.e.*, the discharge pulse duration) for different values of the capacitor bank charging voltage.

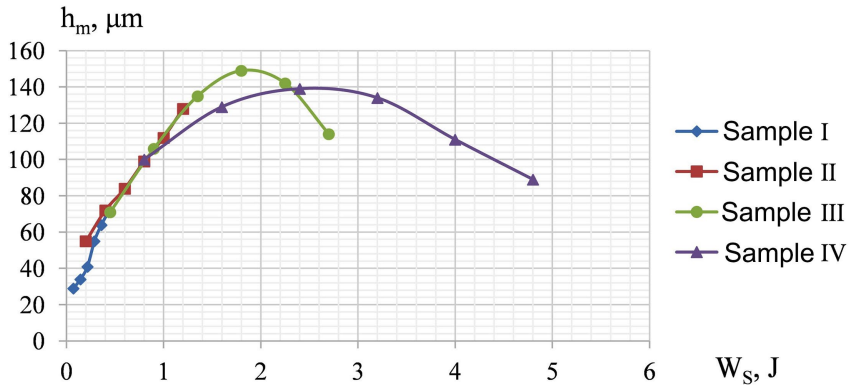

Figure 7. The height of conical meniscus as a function of the energy released in the interstice at different capacities of the generator's capacitor battery.

For Sample I (the energetic parameters of all four samples are shown in Figure 7), the meniscus height increases almost linearly with increasing energy. A similar trend is observed for Sample II. At higher energy levels (Samples III and IV), the height of the Taylor cones initially increases with energy but then decreases significantly beyond a certain value (Figure 7). This behavior can be explained by the fact that a larger portion of energy is transferred to the electrodes, leading to the removal of a certain amount of material from the perturbed metal surface before the menisci are fully formed. In other words, the initial volume of molten, perturbed metal decreases.

To compare experimental data with theoretical models, we plotted the relationship between discharge gap energy and meniscus height.

The duration of the discharge pulse also plays a key role. When the pulse duration is $\tau < 10$ μs, nearly 90% of the metal is removed in vapor form. As the pulse duration increases, the proportion of metal removed as vapor decreases. Thus, in the analysed cases, material removal occurs not only in vapor form but also in

liquid form. Experimental observations confirmed that the discharge pulse duration has a significant influence on meniscus height. It was established that for constant pulse duration, the height of the menisci (Taylor cones) increases with the energy released in the interstice. Conversely, when the energy is kept constant and the pulse duration is varied, the same trend is observed: the meniscus height on the anode surface increases with pulse duration (see Figure 8). This behavior is attributable to process inertia, governed by the intrinsic material properties of the electrode and the duration of the applied electric field. Likewise, maintaining a constant pulse duration while increasing the energy stored in the capacitor bank yields an identical response (Figure 8).

As illustrated in Figures 6-8, discharge energy and pulse duration serve as decisive parameters governing meniscus formation on metallic surfaces. These empirical findings can be attributed to the elevated positioning of the electrode spots relative to the treated substrate, where the pulsed discharge plasma column interacts with the surface. Concurrently, the magnitude of the discharge current remains a function of the target material's intrinsic properties.

The increase in the base diameter of the menisci, observed when the discharge pulse duration is held constant while the stored energy increases, can be attributed to the expansion of the discharge channel. This expansion, in turn, enlarges the electrode spots, which form the connection between the plasma channel and the anode surface. The formation, orientation, and dimensions of the menisci under solitary discharge conditions provide direct evidence that they are not caused by pressure drops in the plasma channel, but rather by the action of the electric field along the vector radius from the electrode spot toward the processed surface of the workpiece.

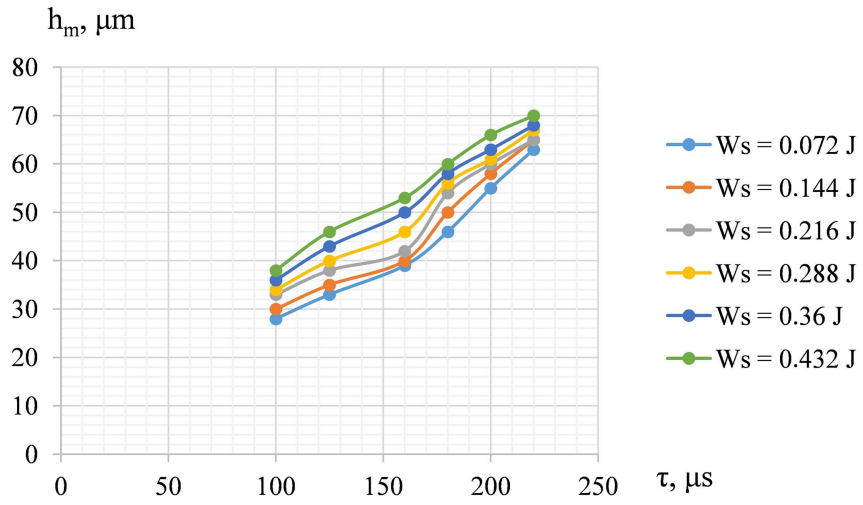

Figure 8. Dependence of meniscus height on discharge pulse duration (S = 0.2 mm) [36].

Experimental investigations revealed that the number and size of conical asperities also depend on the irregularities present on the surfaces of both electrodes, as well as on their shape and dimensions. This was demonstrated by the following

experiment: in two cases, the same base material was used for the tool electrodes. The first electrode had the form of a standard cylinder (flat end), while the second was the same cylinder sharpened to a tip with an apex angle of 30˚. The tool electrodes were connected in the discharge circuit as the anode (although they are typically used as the cathode) under identical energy conditions.

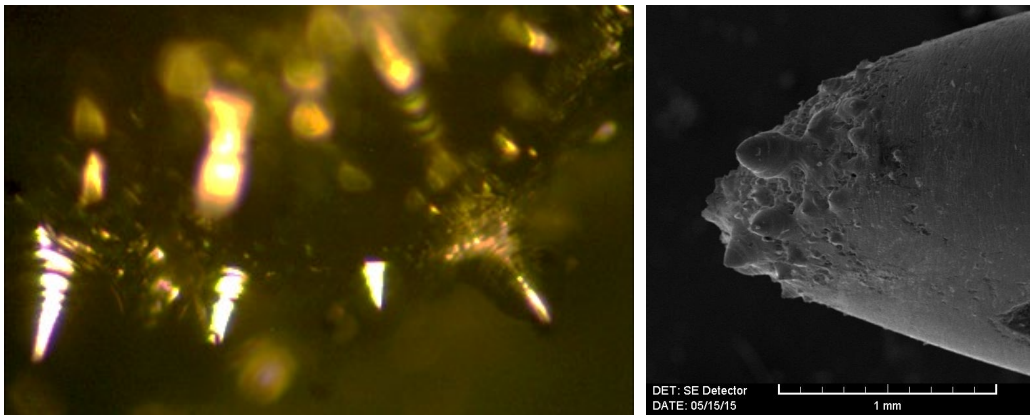

(a) (b)

Figure 9. Cylindrical tool electrode with sharpened tip, connected as anode: (a) optical microscope image; (b) SEM image of the same tip.

The tool electrodes were made of W + Re 20%. The charging voltage of the capacitor bank was U_C = 240 V, the capacitance was set to C = 600 μF, and the initial interelectrode gap was adjusted to S = 0.3 mm. Both the tool and the sample had diameters of 4 mm, and the number of discharge pulses was set to n = 10. As a result, on the sharpened tool electrode connected as the anode (see **Figure 9**), a multitude of large conical asperities were formed, covering almost the entire sharpened tip of the electrode. In contrast, on the flat-ended electrode connected as the cathode, hemispherical craters with much smaller asperities in their centers were observed (see **Figure 10**).

Importantly, no asperities of dimensions comparable to those obtained on the sharpened electrode surfaces were detected. From this, it can be concluded that conical asperities can form on the surfaces of both electrodes (both anode and cathode). However, the asperities extracted on the anode surface are significantly larger. Thus, conical asperities can be produced by pulsed electrical discharges (PED) on all electrically conductive surfaces, regardless of electrode polarity; nevertheless, as mentioned, the effect is more pronounced on anode surfaces. With respect to surface geometry, it is evident that extracting conical asperities is more difficult on flat surfaces than on cylindrical ones. This is largely due to the distribution of the electric field between the electrodes. In experiments aimed at producing conical asperities on flat samples, it was important to maintain both current density and minimal cathode area. After numerous trials at different energy levels released in the interstice, the most successful asperity formation occurred when cylindrical wire tool electrodes with a diameter of 0.2 mm were used.

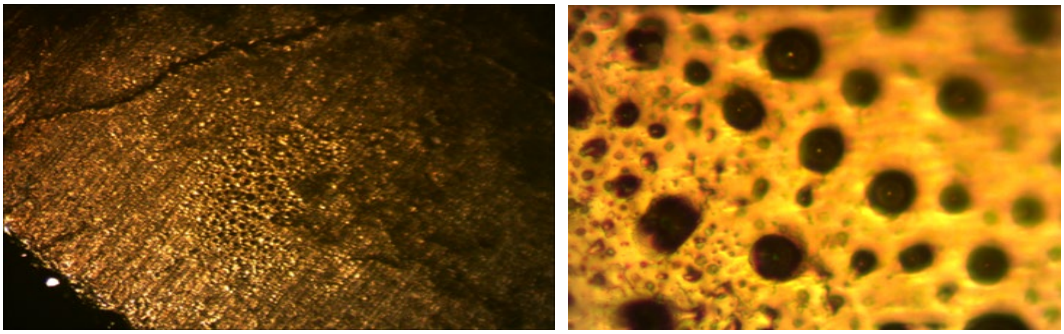

(a) (b)

Figure 10. Cylindrical tool electrode with flat end, connected as cathode: (a) optical magnification 10×; (b) optical magnification 40×.

To derive mathematical relationships for the formation of conical asperities, the discharge pulse duration (ranging from 100 to 220 μs), the interelectrode gap (ranging from 0.1 to 0.4 mm), and the energy released in the interstice (ranging from 0.072 to 4.8 J) were considered. The heights and base diameters of the conical asperities formed on metallic samples made of *W* or *W*-Re alloys containing 10% and 20% Re were measured. The least-squares method was applied, and the experimental data were expressed in logarithmic coordinates, resulting in the following diagrams (see **Figure 11** and **Figure 12**).

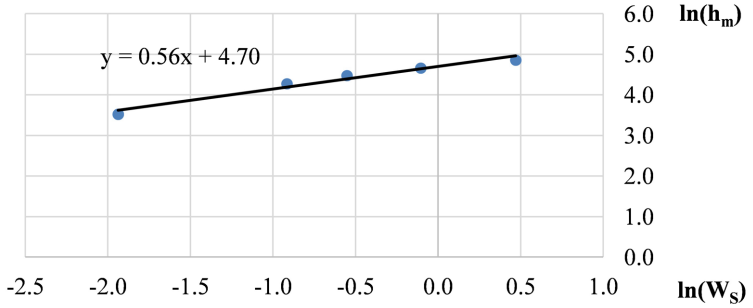

Figure 11. Dependence of asperity height (h_m) on the energy released in the interstice (W_s) in logarithmic values; workpiece electrode made of tungsten wire with a diameter of 0.2 mm. S = 0,2 mm; τ = 125 μs.

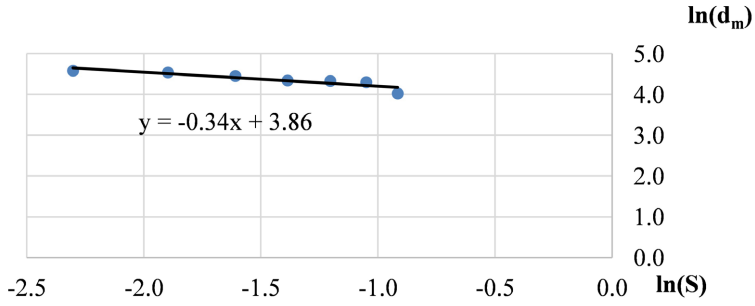

Figure 12. Dependence of asperity base diameter (d_m) on the interelectrode gap (S) in logarithmic values; workpiece electrode made of tungsten wire with a diameter of 0.2 mm; τ = 160 μs; W_s = 0.216 J.

Analyzing the experimental data on conical asperity formation, the following relationships were obtained for average values within the optimal processing ranges [59]:

1) For cathodes made of tungsten wires with diameters of 0.2 and 0.25 mm:

$$h_m = 0.77 \cdot W_S^{0.56} \cdot \tau^{0.88} \cdot S^{-0.34} \quad (3)$$

$$d_m = 2.08 \cdot W_S^{0.46} \cdot \tau^{0.85} \cdot S^{-0,34} \quad (4)$$

2) For cathodes made of tungsten—10% rhenium alloy wires with diameters of 0.2 and 0.25 mm:

$$h_m = 0.66 \cdot W_S^{0.51} \cdot \tau^{0.88} \cdot S^{-0.34} \quad (5)$$

$$d_m = 1.32 \cdot W_S^{0.35} \cdot \tau^{0.85} \cdot S^{-0.34} \quad (6)$$

Relationships (5) and (6) also hold for cathodes made of tungsten—20% rhenium alloy wires with diameters of 0.2 and 0.25 mm.

From these two sets of equations, it can be established that the interelectrode gap (S) and pulse duration (τ) affect the values of h_m and d_m in the same way, regardless of the electrode material composition. However, when considering the released energy and the proportionality coefficient, these values are significantly higher for pure tungsten electrodes, which can be explained by tungsten's higher melting point compared to tungsten-rhenium alloys.

Beyond the study of conical asperity formation on electrode surfaces, the present dissertation also includes attempts to increase the number of asperities, results related to the deoxidation of meniscus surfaces [36], electrode shape modification, and investigations into microsoldering of cylindrical wires made of technical-grade tungsten and its alloys with 10% and 20% rhenium.

Figure 13 shows experimental results on the formation of surfaces with prescribed microgeometry, including cases where conical asperities were extracted under solitary and multiple discharges. It should be noted that it is possible to obtain not only a single meniscus on metallic surfaces, particularly on cylindrical wires (**Figure 13(a)**), but also multiple conical menisci (**Figures 13 (b)-(d)**). The number, dimensions, and shape of these structures largely depend on the discharge energy parameters, interelectrode gap, and electrode positioning.

In **Figure 13(a)**, a single conical asperity formed under the following conditions: released energy W_S = 0.144 J (capacitor bank charging voltage U = 60 V, capacitance C = 200 μF), interelectrode gap S = 0.3 mm, workpiece electrode diameter d_p = 0.25 mm, tool electrode diameter d_s = 0.2 mm, and number of discharges n = 1. The twin-like conical asperities in **Figure 13(b)** formed under the following parameters: W_S = 0.144 J (capacitor bank charging voltage U = 60 V, capacitance C = 200 μF), interelectrode gap S = 0.2 mm, workpiece electrode diameter d_p = 0.25 mm, tool electrode diameter d_s = 0.2 mm, the number of discharge pulses n = 1. In **Figure 13(c)**, asperities were obtained under the same regime as in **Figure 13(b)**, except with an interelectrode gap of S = 0.25 mm. Here, the two asperities differ significantly: the left one is several times smaller than its

neighbour on the right (see Figure 13(c)).

An interesting case is shown in Figure 13(d), where at least four Taylor-type conical asperities are visible: two medium-sized asperities in the centre and two smaller ones on the sides. This structure formed under the following conditions: W_S = 0.256 J (capacitor bank charging voltage U = 80 V, capacitance C = 200 μF), interelectrode gap S = 0.3 mm, the workpiece electrode diameter was d_p = 0.25 mm, the tool electrode diameter was d_s = 0.2 mm, and the number of discharge pulses was n = 1.

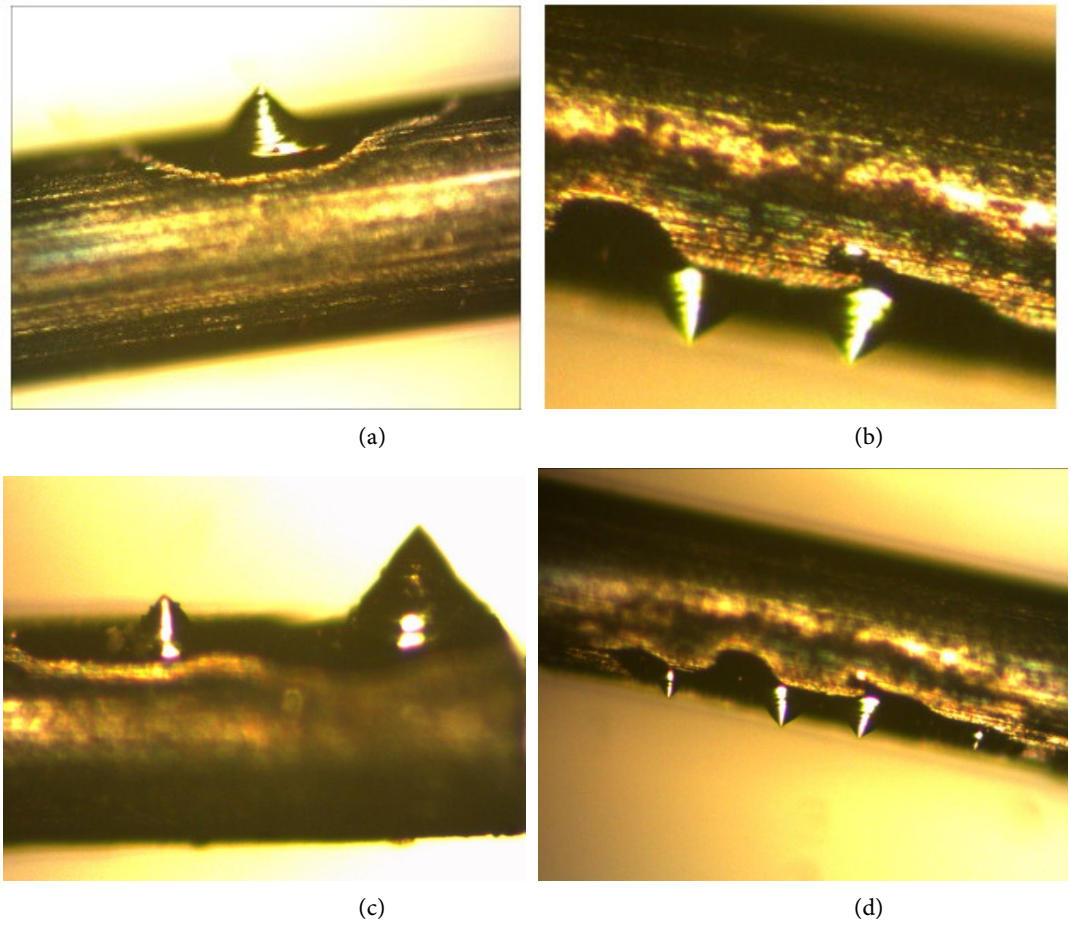

(a) (b)

(c) (d)

Figure 13. General view of menisci extracted from cylindrical sample surfaces [36]: (a) one asperity; (b) and (c) two asperities; (d) four asperities.

Thus, at interelectrode gap values between 0.2 - 0.25 mm, the probability of obtaining multiple conical asperities under solitary discharges increases. Experimental measurements of thermionic electron emission were carried out for different cathodes, whose active surface areas varied depending on whether circular surfaces contained conical menisci or not.

Tables 3-5 present the experimental values of the base diameter and height of the conical menisci, as a function of the surface processing regime, for samples made of technical-grade tungsten and tungsten-rhenium alloys (10% Re or 20%

Re). Based on these results, the increase in active surface area (ΔA) was approximately, yet sufficiently accurately, determined by extracting from it one asperity modelled as a Taylor cone. For this purpose, the asperities were idealized as regular cones, which in practice is only an approximation.

Table 3. Variation of active surface area for thermionic cathodes made of *W* [59].

Nr.	U_c, V	W_S, J	τ, μs	h_m, μm	$d_{b.m.}$, μm	ΔA, μm²
1.	60	0,18	100	28	56	1206,47
2.	60	0,36	125	35	84	1991,94
3.	60	0,54	160	42	112	2945,88
4.	60	0,72	180	56	140	5154,53
5.	60	0,90	200	63	168	6628,23
6.	60	1,08	220	70	182	8133,43

Table 4. Variation of active surface area for thermionic cathodes made of *W*-10% Re alloy [59].

Nr.	U_c, V	W_S, J	τ, μs	h_m, μm	$d_{b.m.}$, μm	ΔA, μm²
1.	60	0,18	100	49	84	3493,33
2.	60	0,36	125	70	84	6049,79
3.	60	0,54	160	84	112	9190,21
4.	60	0,72	180	98	140	12925,69
5.	60	0,90	200	112	168	17259,69
6.	60	1,08	220	126	196	22193,96

Table 5. Variation of active surface area for thermionic cathodes made of *W*-20% Re alloy [36].

Nr.	U_c, V	W_S, J	τ, μs	h_m, μm	$d_{b.m.}$, μm	ΔA, μm²
1.	60	0,18	100	50	86	3642.12
2.	60	0,36	125	71	88	6329.61
3.	60	0,54	160	83	116	9177.37
4.	60	0,72	180	97	143	12846.26
5.	60	0,90	200	111	169	17064.58
6.	60	1,08	220	124	194	21547.98

It was observed that the increase in active area is greater for samples made of tungsten-rhenium alloys. By analysing the data presented in **Table 4** and **Table 5**, it becomes evident that the increase in active area is approximately the same for both *W*-10% Re and *W*-20% Re alloys.

For technical-grade tungsten cathodes, as the energy released in the interstice increased (from 0.18 to 1.08 J), the meniscus height varied from 28 μm to 70 μm,

while the asperity base diameter ranged from 56 μm to 182 μm. For cathodes made of tungsten-rhenium alloys processed under the same conditions, the meniscus height varied from 49 μm to 126 μm, while the asperity base diameter ranged from 84 μm to a maximum of 196 μm. The fact that higher menisci are obtained on the surfaces of tungsten-rhenium alloys compared to pure tungsten surfaces can be explained by the so-called *"rhenium effect."* Empirical observations confirm that the morphological dimensions of the menisci—specifically height and base diameter—exhibit a strong correlation with the energy released in the working gap. Therefore, single-pulse energy input is fundamental to driving meniscus development on treated metal substrates.

4. Conclusions

In light of the present experimental results and previous research in the field, we draw the following conclusions:

1) Surface processing by means of pulsed electrical discharges represents an advanced and efficient method for the controlled modification of the microgeometry and chemical composition of conductive materials, with direct applicability in micro- and nanoelectronics, as well as in the machine- and instrument-building industries.

2) It has been demonstrated that the formation of craters and conical asperities (Taylor cones) is essentially influenced by the operating regime of the pulsed discharge machining (PDM), including pulse energy, interelectrode gap size, electrode connection polarity, and, not least, the material properties of the samples. These conical structures play a crucial role in increasing the active surface area and in enhancing the electron emission phenomena, as demonstrated in [36].

3) A promising research direction has been identified: the establishment of an optimal technological regime for obtaining stable and reproducible conical structures, with a functional role in improving the efficiency of emission, absorption, and radiation-matter interaction processes.

4) The formation of conical asperities is observed on both anode and cathode surfaces; however, they differ in size, with those formed on the anode being larger. For this reason, the workpiece is connected as the anode when surface morphology modification is targeted.

5) The key parameters influencing the geometry of the menisci (Taylor cones) in the course of microgeometry modification of metallic surfaces are the discharge energy, pulse duration, interelectrode gap size, and the material properties of the electrode samples.

Conflicts of Interest

The authors declare no conflicts of interest regarding the publication of this paper.

References

[1] Rusnac, V. (2008) Modification of the Surface Microgeometry of Workpieces during

the Formation of Deposited Layers by the Electroerosion Method. Ph.D. Thesis, Galati, 56 p.

[2] Topala, P., Guzgan, D. and Pleşco, I. (2019) Conditions of Formation of Taylor Cone Shaped Asperities on Metal Surfaces by the Action of PEDM. *AIP Conference Proceedings*, **2075**, Article 060013. https://doi.org/10.1063/1.5091191

[3] Wilson, P. (2007) Formation of Taylor Cones on a Molten Metal Surface Followed by Ion Injection into the Vacuum. SLAC. https://www.slac.stanford.edu/econf/C070523/talks/HG07_talk_Wilson(R).pdf

[4] Suvorov, V.G. and Zubarev, N.M. (2003) Formation of the Taylor Cone on the Surface of Liquid Metal in the Presence of an Electric Field. *Journal of Physics D: Applied Physics*, **37**, 289-297. https://doi.org/10.1088/0022-3727/37/2/019

[5] Talian, I., Mogensen, K.B., Oriňák, A., Kaniansky, D. and Hübner, J. (2009) Surface-enhanced Raman Spectroscopy on Novel Black Silicon-Based Nanostructured Surfaces. *Journal of Raman Spectroscopy*, **40**, 982-986. https://doi.org/10.1002/jrs.2213

[6] Topala, P. and Stoicev, P. (2008) Technologies for Machining Conductive Materials Using Pulsed Electrical Discharges. Tehnica-Info, 265 p.

[7] Topala, P., Guzgan, D., Rusnac, V., Ojegov, A. and Besliu, V. (2015) Specifics of Surface Micro-Geometry Modification under the Action of Temperature and Electric Field of Electrode Spots. *Applied Mechanics and Materials*, **809**, 399-404. https://doi.org/10.4028/www.scientific.net/amm.809-810.399

[8] Tajmar, M. (2005) Influence of Taylor Cone Size on Droplet Generation in an Indium Liquid Metal Ion Source. *Applied Physics A*, **81**, 1447-1450. https://doi.org/10.1007/s00339-005-3207-3

[9] Huang, C., Zhang, H., Chen, S., Lin, J., Qu, X., Zhou, C., *et al.* (2024) Dynamic Simulation of Ion Evaporation from a Conductive Meniscus, Fluid-Fluid Model of Plume and Meniscus Interactions. *Physics of Fluids*, **36**, Article 122108. https://doi.org/10.1063/5.0239989

[10] Cheng, J., Yang, L., Fu, Q., Ren, J., Tang, H., Sun, D., *et al.* (2022) Pulsating Modes of a Taylor Cone under an Unsteady Electric Field. *Physics of Fluids*, **34**, Article 012007. https://doi.org/10.1063/5.0075250

[11] Dong, M., Chen, P., Hang, T. and Li, M. (2021) Nanotwinned Copper Micro-Cone Array Fabricated by Pulse Electrodeposition for Low-Temperature Bonding. *Materials Letters*, **290**, Article 129470. https://doi.org/10.1016/j.matlet.2021.129470

[12] Zhang, M., Gao, L., Wang, Y., Dong, W., Zhao, N. and Liu, Z. (2024) Micro-Cones Cu Fabricated by Pulse Electrodeposition for Solderless Cu-Cu Direct Bonding. *Applied Surface Science*, **650**, Article 159184. https://doi.org/10.1016/j.apsusc.2023.159184

[13] Higuera, F.J. (2003) Flow Rate and Electric Current Emitted by a Taylor Cone. *Journal of Fluid Mechanics*, **484**, 303-327. https://doi.org/10.1017/s0022112003004385

[14] Gamero-Castaño, M. and Cisquella-Serra, A. (2021) Electrosprays of Highly Conducting Liquids: A Study of Droplet and Ion Emission Based on Retarding Potential and Time-of-Flight Spectrometry. *Physical Review Fluids*, **6**, Article 013701. https://doi.org/10.1103/physrevfluids.6.013701

[15] Rajput, V., Goud, M. and Suri, N.M. (2021) Multi-Spark Simulation of the Electrochemical Discharge Machining (ECDM) Process. *Journal of Mechanical Science and Technology*, **35**, 5127-5135. https://doi.org/10.1007/s12206-021-1029-7

[16] Ferreira, J.C. (2006) A Study of Die Helical Thread Cavity Surface Finish Made by

Cu-W Electrodes with Planetary EDM. *The International Journal of Advanced Manufacturing Technology*, **34**, 1120-1132. https://doi.org/10.1007/s00170-006-0687-z

[17] Topala, P. (2008) Fundamental and Applied Study of Electroerosive Effects in Non-Conventional Technologies. Abstract of the Habilitation Thesis in Engineering. Tehnica UTM, 51 p.

[18] Topala, P. and Guzgan, D. (2013) The Technology of Surface Micro Geometry Modifications via Application of Electric Discharges in Impulse. *Advanced Manufacturing Technologies*, Sozopol, 26-30 June 2013, 97-104.

[19] Tiginyanu, I., Topala, P. and Ursaki, V. (2016) Nanostructures and Thin Films for Multifunctional Applications: Technology, Properties and Devices. Springer, 576 p.

[20] Topala, P., Olaru, I. and Rusnac, V. (2005) New Sequences in the Physical Picture of the Electroerosion Phenomenon. *Collection of Scientific Papers*: *Modern Technologies*, *Quality*, *Restructuring*, **2**, 299-302.

[21] Stavitskii, B.I. (2002) Spark-Erosion Precision Machining of Materials: Scientific Foundations of Ultra-Precision Surface-Forming Methods. *Electronic Processing of Materials*, **38**, 5-32.

[22] Rusnac, V. and Guzgan, D. (2010) Influence of the Magnetic Field on the Formation of Taylor Cones during Electro-Pulse Processing of Metals. *Mechanical Engineering and Technosphere of the* 21*st Century*: *Proceedings of the XVII International Scientific and Technical Conference*, **3**. 67-72.

[23] Guzgan, D. (2014) The Results on Metal Surface Micro Geometry Modification by Applying Electric Discharges in Impulse. *ACTA Universitatis Cibiniensis*, **65**, 32-38. https://doi.org/10.1515/aucts-2015-0006

[24] Topala, P., Ojegov, A., Harbu, A., Besliu, V. and Guzgan, D. (2019) Physical and Chemical Phenomena at the Interaction of EDI Plasma with Electrodes Surfaces. *AIP Conference Proceedings*, **2075**, Article 060012. https://doi.org/10.1063/1.5091190

[25] Safronov, I.I., Topala, P.A. and Gorbunov, A.S. (2009) Electro-Erosion Processes on the Electrodes and Micro-Structural and Phase Composition of Alloying Strata. Tehnica-Info, 495 p.

[26] Kirko, D.L. and Savjolov, A.S. (2017) Properties of Plasma in Case of Capillary Discharge Interaction with Metals. *Journal of Physics*: *Conference Series*, **941**, Article 012017. https://doi.org/10.1088/1742-6596/941/1/012017

[27] Topala, P., Besliu, V., Rusnac, V., Ojegov, A. and Pinzaru, N. (2011) Structural Modification of the Chemical Composition and Microgeometry of Part Surfaces through the Application of Pulsed Electrical Discharges (PED). *Physics and Technology*: *Processes*, *Models*, *Experiments*, No. 1, 36-42. https://ibn.idsi.md/ro/vizualizare_numar_revista/99/1378

[28] Krasnova, E.V., Morgunov, Y.A. and Saushkin, B.P. (2022) Statistical Investigation of the Surface Roughness of Ti-6Al-4V Products Built by Selective Electron Beam Melting. *Elektronnaya Obrabotka Materialov*, **58**, 1-12. https://doi.org/10.52577/eom.2022.58.6.01

[29] Yu, S.F., Lee, B.Y. and Lin, W.S. (2001) Waveform Monitoring of Electric Discharge Machining by Wavelet Transform. *The International Journal of Advanced Manufacturing Technology*, **17**, 339-343. https://doi.org/10.1007/s001700170168

[30] Guzgan, D. (2015) Imparting a Prescribed Microgeometry to Metal Surfaces to Enhance the Intensity of Thermionic Emission Current. *Proceedings of the Conference* '*Science and Innovation in Northern Moldova*: *Challenges*, *Achievements*, *Perspectives*', Bălți, 25-26 September 2015, 21-23.

https://ibn.idsi.md/ro/vizualizare_articol/136701

[31] Guzgan, D. (2016) Modification of the Cathode Surface Microgeometry to Enhance the Intensity of Thermionic Emission Current. *Proceedings of the International Scientific Conference*: *Relevance and Quality of University Education*: *Competences for the Present and the Future*, **1**, 142-144. http://dspace.usarb.md:8080/jspui/bitstream/123456789/2341/1/Guzgan_modificarea_suprafetei.pdf

[32] Topala, P., Rusnac, V. and Guzgan, D. (2012) Increasing the Thermoelectric Capacity of Emition in Cathodes by Modifying Their Surface Microgeometry. *The* 16*th International Conference Inventica*, Iasi, 13-15 June 2012, 623-624.

[33] Benea, L., Başa, S., Dănăilă, E., Caron, N., Raquet, O., Ponthiaux, P., *et al*. (2015) Fretting and Wear Behaviors of Ni/Nano-WC Composite Coatings in Dry and Wet Conditions. *Materials & Design*, **65**, 550-558. https://doi.org/10.1016/j.matdes.2014.09.050

[34] Mesyats, G.A. (1995) Ecton or Electron Avalanche from Metal. *Physics-Uspekhi*, **38**, 567-590. https://doi.org/10.1070/pu1995v038n06abeh000089

[35] Giubileo, F., Di Bartolomeo, A., Iemmo, L., Luongo, G. and Urban, F. (2018) Field Emission from Carbon Nanostructures. *Applied Sciences*, **8**, Article 526. https://doi.org/10.3390/app8040526

[36] Guzgan, D. (2024) Research on the Increasing Capacity of the Thermo-Electronic Emission of Metallic Surfaces by Electro-Erosion Method. Ph.D. Thesis, Technical University of Moldova, 35.

[37] Topala, P., Guzgan, D. and Plesco, I. (2019) Increasing the Surface Thermo-Emission by the Formation of Asperities of Taylor Cone Type. In: Naito, M., Buchacz, A., Baier, A., Topala, P. and Nedelcu, D., Eds., *Research and Innovation in Advanced Engineering Materials*, ModTech Publishing House, 159-184.

[38] Mesyats, G.A. (2011) Explosive Electron Emission. Fizmatlit, 280 p.

[39] Pavel, T., Nicolae, I., Laurentiu, S., Alexandr, O., Ghiculescu, D., Laurentiu, M., *et al*. (2024) Complex Physical Phenomenology of EDM with Technological Applications. In: Nagata, K., Ed., *Current Research Progress in Physical Science*, Vol. 6, BP International, 1-36. https://doi.org/10.9734/bpi/crpps/v6/3390

[40] Topala, P., Rusnac, V., Guzgan, D., Plesco, I. and Ojegov, A. (2013) Experimental Research on the Extraction of Conical Menisci from Metal Surfaces and Their Oxidation Using Pulsed Electric Discharges. *Fizică şi Tehnică*: *Procese*, *Modele*, *Experimente*, No.1, Balti, 40-43. https://ibn.idsi.md/ro/vizualizare_articol/38692

[41] Topala, P., Hirbu, A. and Ojegov, A. (2012) The Action of Electric Discharge Plasma on Metal Surfaces. *Physics and Modern Technologies*, **10**, 13-21. https://ibn.idsi.md/sites/default/files/j_nr_file/vol10_2012.pdf

[42] Topala, P., Ojegov, A., Besliu, V., Rusnac, V., Guzgan, D., Hirbu, A. and Plesco, I. (2015) Oxidation of Taylor Cone-Shaped Asperities by Application of Plasma in Normal Condition. *Nonconventional Technologies Review*, **19**, 56-61. http://dspace.usarb.md:8080/jspui/bitstream/123456789/3167/1/Topala_oxidation.pdf

[43] Grigoryev, A.I., Shiryaeva, S.O., Belonozhko, D.F. and Klimov, A.V. (2004) About the Shape of the Taylor Cone and the Characteristic Time of Its Growth. *Electronic Processing of Materials*, **40**, 34-40.

[44] Belyaev, M.A., Zubarev, N.M. and Zubareva, O.V. (2019) Conical Structures on the Surface of a Liquid with Ion Current in the Space-Charge Limited Mode. 2019 *IEEE*

20*th International Conference on Dielectric Liquids* (*ICDL*), Roma, 23-27 June 2019, 1-4. https://doi.org/10.1109/icdl.2019.8796820

[45] Suvorov, V.G. and Litvinov, E.A. (2000) Dynamic Taylor Cone Formation on Liquid Metal Surface: Numerical Modelling. *Journal of Physics D: Applied Physics*, **33**, 1245-1251. https://doi.org/10.1088/0022-3727/33/11/301

[46] Topala, P., Guzgan, D. and Rusnac, V. (2013) Surface Formation Technologies for Electronic Emission. *Scientific Papers: Agricultural Engineering and Automotive Transport*, **38**, 196-201.

[47] Topala, P., Rusnac, V. and Guzgan, D. (2014) Formation of Taylor Cone Shaped Asperities on Cylindrical Surfaces by Applying Electric Discharges in Pulse. *Advanced Materials Research*, **1036**, 178-183. https://doi.org/10.4028/www.scientific.net/amr.1036.178

[48] Balan, N.N., Ivashov, E.N., Luchnikov, P.A. and Nevskii, A.B. (2012) Field-Emission Electron Emitters for Microdevices and Technological Features of Their Fabrication. *Vestnik Nauki Sibiri* (*Siberian Journal of Science*), **3**, 89-98.

[49] Zhang, J., Cai, G., Liu, X., He, B. and Wang, W. (2021) Molecular Dynamics Simulation of Ionic Liquid Electrospray: Revealing the Effects of Interaction Potential Models. *Acta Astronautica*, **179**, 581-593. https://doi.org/10.1016/j.actaastro.2020.11.018

[50] Rotaru, N., Maliga, O. and Codreanu, I. (2020) Radiology and Radiation Protection. CEP Medicina, 242 p.

[51] Balan, N.N. and Ivashov, E.N. (2012) Prospective Electrode Materials for Autoemission and Tunnel Microdevices. *Proceedings of the International Scientific and Practical Conference* "*Info*-2012", Sochi, 1-10 October, 2012, 319-325.

[52] Topala, P., Besliu, V., Rusnac, V., Guzgan, D. and Pleco, I. (2014) Obtaining Surfaces with Taylor Cone Shaped Asperities of Micro- and Nano-Scale Dimensions Using the EDI Method. *International Journal of Modern Manufacturing Technologies*, **6**, 91-96. https://ijmmt.ro/vol6no22014/Topala_Pavel.pdf

[53] Zhang, Y., Liu, Y., Shen, Y., Li, Z., Ji, R. and Cai, B. (2014) A Novel Method of Determining Energy Distribution and Plasma Diameter of EDM. *International Journal of Heat and Mass Transfer*, **75**, 425-432. https://doi.org/10.1016/j.ijheatmasstransfer.2014.03.082

[54] Rusnac, V. (2008) The Role of Energy and Duration of Discharging Pulse during the Micro Geometry Changing Process of Metallic Parts Surfaces by Applying Electric Discharges in Impulse. *The Annals of Dunarea de Jos University of Galati, Fascicle V, Technologies in Machine Building*, **1**, 61-68,

[55] Topala, P., Guzgan, D. and Rusnac, V. (2014) Experimental Research on the Modification of Metal Workpiece Surface Geometry. *Colloquium* "*Tradition and Innovation in Scientific Research*", Balti, 18 October 2013, 250-255. https://ibn.idsi.md/ro/vizualizare_articol/99302

[56] Pinzaru, N. (2020) Research on the Design, Development, and Fabrication of "Tool Electrodes" for Surface Layer Formation Using Pulsed Electrical Discharges. Doctoral Thesis, Universitatea Tehnică a Moldovei, 26 p.

[57] Neagu, D. (2007) Applications of the Electron Beam. 26 p. http://www.dumitruneagu.ro/pdf/(6.3.2)APLICATIIale%20FE.pdf

[58] Topala, P. (2007) Electrical Charges as Measures for Removed Metal Mass the Electrical Discharge Machining. *Nonconventional Technologies Review*, No. 4, 103-108.

[59] Topala, P., Dorin, G. and Ojegov, A. (2021) Increasing the Energy Efficiency of Thermocathodes Operation. *Global Journal for Research Analysis*, **10**, 164-168.

https://doi.org/10.36106/gjra/4914740

[60] Benea, L. and Danaila, E. (2016) Nucleation and Growth Mechanism of Ni/TiO_2 Nanoparticles Electro-Codeposition. *Journal of The Electrochemical Society*, **163**, D655-D662. https://doi.org/10.1149/2.0591613jes